6484 *Inorg. Chem.* **2010**, *49*, 6484–6494
DOI: 10.1021/ic100170t

Inorganic Chemistry
Article

# Competitive Complexation of Nitrates and Chlorides to Uranyl in a Room Temperature Ionic Liquid

**C. Gaillard,*,† A. Chaumont,‡ I. Billard,§ C. Hennig,∥ A. Ouadi,§ S. Georg,§ and G. Wipff*,‡**

†*Institut de Physique Nucléaire de Lyon, CNRS-IN2P3, 4 rue Enrico Fermi, 69622 Villeurbanne cedex, France,* ‡*Laboratoire MSM, UMR 7177, Institut de Chimie, 4 rue B. Pascal, 67000 Strasbourg, France,* §*Institut Pluridisciplinaire Hubert Curien, DRS, Chimie Nucléaire, 23 rue du Lœss, 67037 Strasbourg cedex 2, France, and* ∥*Institute of Radiochemistry, Forschungszentrum Dresden-Rossendorf, P.O. Box 510119, 01314 Dresden, Germany*

Received January 28, 2010

By coupling EXAFS, UV−vis spectroscopy, and molecular dynamics and quantum mechanical calculations, we studied the competitive complexation of uranyl cations with nitrate and chloride ions in a water immiscible ionic liquid (IL), $C_4mimTf_2N$ ($C_4mim^+$: 1-butyl-3-methyl-imidazolium; $Tf_2N^-$ = $(CF_3SO_2)_2N)^-$: bis(trifluoromethylsulfonyl)imide). Both nitrate and chloride are stronger ligands for uranyl than the IL $Tf_2N^-$ or triflate anions and when those anions are simultaneously present, neither the limiting complex $UO_2(NO_3)_3^-$ nor $UO_2Cl_4^{2-}$ alone could be observed. At a $U/NO_3/Cl$ ratio of 1/2/2, the dominant species is likely $UO_2Cl(NO_3)_2^-$. When chloride is in excess over uranyl with different nitrate concentrations ($U/NO_3/Cl$ ratio of 1/2/6, 1/4/4, and 1/12/4) the solution contains a mixture of $UO_2Cl_4^{2-}$ and $UO_2Cl_3(NO_3)^{2-}$ species. Furthermore, it is shown that the experimental protocol for introducing these anions to the solution (either as uranyl counterion, as added salt, or as IL component) influences the UV−vis spectra, pointing to the formation of different kinetically equilibrated complexes in the IL.

## Introduction

Room temperature ionic liquids (ILs) are composed of an anionic and a cationic part that both influence their physicochemical properties like viscosity, hygroscopy, miscibility with other solvents, and electrochemical behavior. It should thus be possible to tune the physicochemical properties of ILs for a given chemical application.[1−4] Moreover, ILs are easy to handle at room temperature and display environmentally wished characteristics as they are stable under air and water and not volatile. This explains the keen interest in ILs over the past decade in many fields of chemistry. Because of their rather good radiolytic stability,[5−7] ILs emerge as interesting media for nuclear fuel reprocessing,[8] either in replacement of volatile organic solvents for liquid−liquid partitioning of actinides and lanthanides[9−11] or as complexing agents in the case of "task specific ILs" where complexing moieties are grafted on the IL anion or cation.[1,12] It was shown that uranyl chloro complexes formed in those media are the same as in other solvents like acetone or acetonitrile.[13,14] However, considering ILs as only "green" surrogates for organic solvents would be too simplistic as they have an influence on chemical processes. For instance, while $Ln^{(III)}$ lanthanides and $An^{(III)}$ actinides are generally considered as chemical homologues, they behave differently in ILs.[15] Stumpf et al. studied the interactions between $Eu^{(III)}$, $Am^{(III)}$, or $Cm^{(III)}$ with azide ions ($N_3^-$) in the IL $C_4mimTf_2N$ ($C_4mim^+$: 1-butyl-3-methyl-imidazolium; $Tf_2N^-$ = $(CF_3SO_2)_2N)^-$: bis-(trifluoromethylsulfonyl)imide) and observed different kinetics of complexation for $Ln^{(III)}$ and $An^{(III)}$ ions, which

*To whom correspondence should be addressed. E-mail: c.gaillard@ipnl.in2p3.fr.

(1) Lee, S.-G. *Chem. Commun.* **2006**, 1049.
(2) Welton, T. *Chem. Rev.* **1999**, *99*, 2071.
(3) Davis, J. H.; Fox, P. A. *Chem. Commun.* **2003**, 1209.
(4) Dupont, J.; Suarez, P. A. *Phys. Chem. Chem. Phys.* **2006**, *8*, 2441.
(5) Allen, D.; Baston, G. M.; Bradley, A. E.; Gorman, T.; Haile, A.; Hamblett, I.; Hatter, J. E.; Healey, M. J.; Hodgston, B.; Lewin, R.; Lovell, K. V.; Newton, B.; Pitner, W. R.; Rooney, D. W.; Sanders, D.; Seddon, K. R.; Sims, H. E.; Thied, R. C. *Green Chem.* **2002**, *4*, 152.
(6) Berthon, L.; Nikitenko, S.; Bisel, I.; Berthon, C.; Faucon, M.; Saucerotte, B.; Zorz, N.; Moisy, P. *Dalton Trans.* **2006**, 2526.
(7) Bossé, E.; Berthon, L.; Zorz, N.; Monget, J.; Berthon, C.; Bisel, I.; Legand, S.; Moisy, P. *Dalton Trans.* **2008**, 924.
(8) Cocalia, V. A.; Gutowski, K. E.; Rogers, R. D. *Coord. Chem. Rev.* **2006**, *250*, 755.
(9) Dietz, M. L.; Stepinski, D. C. *Talanta* **2008**, *75*, 598.
(10) Jensen, M. P.; Neuefeind, J.; Beitz, J. V.; Skanthakumar, S.; Soderholm, L. *J. Am. Chem. Soc.* **2003**, *125*(50), 15466.
(11) Visser, A. E.; Rogers, R. D. *J. Solid State Chem.* **2003**, *171*, 109.
(12) Ouadi, A.; Klimchuk, O.; Gaillard, C.; Billard, I. *Green Chem.* **2007**, *9*, 1160.
(13) Gaillard, C.; Chaumont, A.; Billard, I.; Hennig, C.; Ouadi, A.; Wipff, G. *Inorg. Chem.* **2007**, *46*, 4815.
(14) Servaes, K.; Hennig, C.; Billard, I.; Gaillard, C.; Binnemans, K.; Görller-Wallrand, C.; Van Deun, R. *Eur. J. Inorg. Chem.* **2007**, No. 32, 5120.
(15) Stumpf, S.; Billard, I.; Gaillard, C.; Panak, P. J.; Dardenne, K. *Radiochim. Acta* **2008**, *96*, 1.

 Published on Web 06/17/2010 © 2010 American Chemical Society

**Table 1.** Complexation of Uranium(VI) with Nitrates in $C_4mimTf_2N$ Solutions: Summary of Samples Composition

| sample ID | uranyl salt and concentration | [TBA-$NO_3$], M | [$UO_2^{2+}$]/[$NO_3^-$] |
|---|---|---|---|
| A | $UO_2(Tf_2N)_2$, 0.02 M | | 1/0 |
| B | $UO_2(Tf_2N)_2$, 0.02 M | 0.02 | 1/1 |
| C | $UO_2(Tf_2N)_2$, 0.02 M | 0.04 | 1/2 |
| D | $UO_2(Tf_2N)_2$, 0.02 M | 0.06 | 1/3 |
| E[a] | $UO_2(Tf_2N)_2$, 0.02 M | 0.08 | 1/4 |
| F | $UO_2(CF_3SO_3)_2$, 0.02 M | 0.02 | 1/1 |
| G | $UO_2(CF_3SO_3)_2$, 0.02 M | 0.04 | 1/2 |
| H | $UO_2(CF_3SO_3)_2$, 0.02 M | 0.06 | 1/3 |

[a] From reference 21.

could not be attributed to the sole effects of the solution viscosity or concentration.[16] They also measured the quenching influence of $Cu^{(II)}$ on the fluorescence emission of $Eu^{(III)}$ and $Cm^{(III)}$ in $C_4mimTf_2N$ by TRLFS. These measurements suggest that the coordination by solvating ligands has a great and different impact on the reactivities of lanthanide and actinide ions.[17] Another case concerns the field of liquid −liquid extraction where ILs are used as receiving phase: the nature of their cationic constituent may influence the nature of extracted species and the extraction mechanism.[18,19]

We have undertaken studies on fundamental chemistry of uranyl in ILs and investigated the coordination sphere of uranyl as a function of the dissolved salt.[13] In particular, we showed that in the IL medium, contrary to water, for example, uranyl interacts with nitrate ions: after dissolution of uranyl nitrate in ILs, the nitrates remain coordinated to uranyl. This contrasts with aqueous solutions where the stabilization of uranyl nitrate complexes requires a high excess of nitrates.[20] Nitrate ions play an important role in nuclear fuel reprocessing where concentrated nitric acid is used to dissolve the spent fuel. The major component of the fuel, $UO_2$, dissolves in an IL ($C_4mimTf_2N$) in the presence of concentrated $HNO_3$ aqueous solution.[21] Dissolution occurs with a change of oxidation state from U(IV) to U(VI) resulting in the complexation with nitrates to form $UO_2(NO_3)_3^-$ species. The stability of this complex in a water-saturated IL is quite unusual and hints of a strong affinity of nitrates for uranyl ions in IL solutions.

We have also investigated by UV−vis and EXAFS spectroscopies the solvation of uranyl salts (nitrate, perchlorate, triflate) in ILs based on a same cation $C_4mim^+$ (1-methyl-3-butylimidazolium$^+$) and different anions ($Tf_2N^-$, $PF_6^-$, $BF_4^-$, $CF_3SO_3^-$) and investigated the effect of added $Cl^-$ anions.[13] Adding a 4-fold excess of chlorides to an uranyl solution in different ILs lead to complete $Cl^-$ complexation to form the limiting $UO_2Cl_4^{2-}$ species, excepted when uranyl was dissolved in the IL as a nitrate salt.[13] In that case, the UV−vis spectrum displayed unusual features, compared to the spectrum of $UO_2Cl_4^{2-}$, suggesting that the chloride complexation was not total and that certain amount of nitrate remained in the coordination shell. This result stimulated us to more extensively study the complexation of nitrates with uranyl and the competition between nitrate and chloride ligands in the hydrophobic IL $C_4mimTf_2N$. The results, based on the analysis of 16 samples (noted A−P; see Table 1) are presented in this paper. Samples A and E, previously studied (by UV−vis and UV−vis + EXAFS, respectively), are included for comparison. We analyze $C_4mimTf_2N$ solutions of uranyl in which chlorides and nitrates were added at different amounts, and by different means. Experimental EXAFS and UV−vis spectroscopic studies have been run in parallel with molecular dynamics simulations on selected systems and by quantum mechanical (QM) calculations, allowing us to conduct an experimental strategy and to gain insights into the solvation and energy features of mixed chloro and nitrato- complexes in the IL.

**Table 2.** Competition between Nitrate and Chloride Ions in $C_4mimTf_2N$ Solution of $UO_2(Tf_2N)_2$ or $UO_2(NO_3)_2$ As a Function of the Nature of Added Salts and $Cl^-$ and $NO_3^-$ Concentrations: Summary of Samples Composition

| sample ID | uranyl salt and concentration | nitrate salt | chloride salt | [$UO_2^{2+}$]/[$NO_3^-$]/[$Cl^-$] |
|---|---|---|---|---|
| I | $UO_2(NO_3)_2$, 0.05 M | | TBA-Cl | 1/2/2 |
| J | $UO_2(NO_3)_2$, 0.05M | | TBA-Cl | 1/2/6 |
| K | $UO_2(Tf_2N)_2$, 0.01 M | | TBA-Cl | 1/0/4 |
| L | $UO_2(Tf_2N)_2$, 0.01 M | | $C_4mimCl$ | 1/0/4 |
| M | $UO_2(Tf_2N)_2$, 0.01 M | TBA-$NO_3$ | $C_4mimCl$ | 1/4/4 |
| N | $UO_2(Tf_2N)_2$, 0.01 M | TBA-$NO_3$ | $C_4mimCl$ | 1/12/4 |
| O | $UO_2(Tf_2N)_2$, 0.01 M | $C_4mimNO_3$ | $C_4mimCl$ | 1/3/4 |
| P | $UO_2(Tf_2N)_2$, 0.01 M | $C_4mimNO_3$ | $C_4mimCl$ | 1/2/6 |

## Methods

**Experiments.** The IL $C_4mimTf_2N$ ($Tf_2N$ = $(CF_3SO_2)_2N^-$ ; purity 99%, [$Cl^-$] < $2 \times 10^{-3}$ M) and $C_4mimCl$ (purity 98%) were purchased from Solvionic. $C_4mimNO_3$ was synthesized according to the procedure described in ref 22, and the other salts were either synthesized in our laboratory,[23] uranyl triflate $UO_2(CF_3SO_3)_2$, $(UO_2)(Tf_2N)_2$, or purchased, uranyl nitrate $UO_2(NO_3)_2 \cdot 6H_2O$ and tetra-butyl-ammonium-nitrate (TBA-$NO_3$) from Fluka, tetra-butyl-ammonium-chloride (TBA-Cl) from Aldrich.

Samples A to J were analyzed by both EXAFS and UV−vis spectroscopies (see compositions in Tables 1 and 2). After dissolution of the salts in the IL, samples were degassed under vacuum at 60 °C for 10 h and were immediately transferred in sealed polyethylene containers for their EXAFS analysis to prevent any water reabsorption. After the EXAFS measurements, solutions were transferred in quartz cells for their UV−vis absorption analysis. UV−vis spectra were recorded at 18 °C on a Varian Cary 100 spectrophotometer between 200 and 700 nm, using an empty quartz cell as reference (optical path length = 1 cm). Samples K to P were studied by UV−vis analysis only a few hours after their preparation. In every case, the UV−vis spectra were checked to be reproducible over several weeks.

The water content of all samples was measured by Karl Fischer titration after recording of EXAFS and UV−vis spectra. It was found below 50 ppm (0.004 M, detection limit of the Karl Fischer technique), which corresponds to less than one water molecule per uranyl cation.

EXAFS experiments were carried out on one-week-old samples at the ROBL-ESRF beamline, at the U $L_{III}$ edge, in transmission mode using argon-filled ionization chambers at ambient temperature. The measurements were performed using

(16) Stumpf, S.; Billard, I.; Gaillard, C.; Panak, P. J.; Dardenne, K. *Inorg. Chem.* **2008**, *47*, 4618.
(17) Stumpf, S.; Billard, I.; Panak, P. J.; Mekki, S. *Dalton Trans.* **2007**, 240.
(18) Dietz, M. L.; Stepinski, D. C. *Green Chem.* **2005**, *7*, 747.
(19) Dietz, M. L.; Dzielawa, J. A.; Laszak, I.; Young, B. A.; Jensen, M. P. *Green Chem.* **2003**, *5*, 682.
(20) Ikeda, A.; Hennig, C.; Tsushima, S.; Scheinost, A. C.; Bernhard, G.; Yaita, T. *Inorg. Chem.* **2009**, *48*, 7201.
(21) Billard, I.; Gaillard, C.; Hennig, C. *Dalton Trans.* **2007**, 4214.
(22) Georg, S.; Billard, I.; Ouadi, A.; Gaillard, C.; Petitjean, L.; Picquet, M.; Solov'ev, V. *J. Phys. Chem. B* **2010**, *114*, 4276.
(23) Bouby, M. University L. Pasteur, Strasbourg, France, 1998.

a double crystal Si(111) monochromator. An yttrium foil was used to calibrate the monochromator energy at 17038 eV. XAFS data reduction was made using the IFEFFIT code.[24] Data analysis was carried out with the FEFFIT code,[25] using phase and backscattering amplitude functions generated with the FEFF 8.1 code[26] from crystal structure data of $UO_2(CF_3SO_3)_2 \cdot 3H_2O$,[27] $Cs_2UO_2Cl_4$,[28] and $UO_2(NO_3)_2(H_2O)_2 \cdot H_2O$.[29] Fits of the Fourier transform (FT) $k^3$-weighted EXAFS data to the EXAFS equation were performed in R-space between 1 and 4.3 Å. The $k$-range used was 3.0−16.8 $Å^{-1}$. The amplitude reduction factor ($S_0^2$) was held constant to 1 for all fits. The shift in the threshold energy ($E_0$) was allowed to vary as a global parameter for all atoms. In all fits, the coordination number of the uranyl axial oxygen atoms ($O_{ax}$) was held constant at two. Multiple scattering paths stemming from the uranyl (axial oxygens) and nitrate (distal oxygens) groups were included in the fit as fixed parameters. The multiple scattering path of the axial oxygens was included in the curve fit by constraining its effective path-length to twice the values of the corresponding U−$O_{ax}$ distance. For the nitrate groups, the number of distal oxygen atoms was defined as equal to the number of nitrogen atoms.

**Molecular Dynamics Simulations.** Selected IL solutions were simulated by classical molecular dynamics using the AMBER 7.0 software[30] in which the potential energy $U$ is described by a sum of bond, angle, and dihedral deformation energy and a pair wise additive 1−6−12 (electrostatic and van der Waals) interaction between non-bonded atoms:

$$U = \sum_{bonds} k_b(r - r_0)^2 + \sum_{angles} k_\theta(\theta - \theta_0)^2 + \sum_{dihedrals} \sum_{n} V_n(1 + \cos(n\varphi - \gamma)) + \sum_{i<j} \left[ \frac{q_i q_j}{R_{ij}} - 2\varepsilon_{ij}\left(\frac{R^*_{ij}}{R_{ij}}\right)^6 + \varepsilon_{ij}\left(\frac{R^*_{ij}}{R_{ij}}\right)^{12} \right] \quad (1)$$

Cross terms in van der Waals interactions were constructed using the Lorentz−Berthelot rules. Force field parameters for the pure IL were taken from the work of Andrade et al.[31] for $C_4mim^+$ while those for $Tf_2N^-$ are from Pádua et al.[32] These parameters have been shown to give good agreement with experimental data for the neat liquids.

The parameters for $UO_2^{2+}$ are those of Guilbaud and Wipff,[33] while those for $NO_3^-$ are taken from the Baaden et al.[34] work on lanthanide complexes. The 1−4 van der Waals interactions were scaled down by 2.0 and the 1−4 Coulombic interactions were scaled down by 2.0 as in ref 35. The pure liquids and solutions were simulated with 3D-periodic boundary conditions. Non-bonded interactions were calculated using a 12 Å atom based cutoff, calculating the long-range electrostatics using the Ewald summation method in the Particle Mesh Ewald (PME) approximation.

MD simulations were performed at 400 K to enhance the sampling, starting with random velocities, using the Verlet leap-frog algorithm with a time step of 2 fs to integrate the equations of motion. The temperature was monitored by coupling the system to a thermal bath using the Berendsen algorithm with a relaxation time of 0.2 ps. All C−H bonds were constrained using the SHAKE algorithm.

We first equilibrated "cubic" boxes of pure liquids at 300 K, of about 45 Å length containing 200 $C_4mim^+$ $Tf_2N^-$ ions. The resulting solvent density (1.49 g/$cm^3$) was in reasonable agreement with experimental data (1.438 g/$cm^3$).[36] We then immersed the different uranyl complexes ($UO_2(NO_3)_2$, $UO_2Cl(NO_3)_2^-$, $UO_2Cl_2(NO_3)_2^{2-}$, $UO_2Cl_3(NO_3)^{2-}$, and $UO_2Cl_4^{2-}$) in the box. Complexed $NO_3^-$ anions were constrained to remain bidentate with U−O bond distances of 2.45 Å and a force constant of 400 kcal $Mol^{-1}$ $Å^2$. Additional free $Cl^-$ and $NO_3^-$ anions were added, at about 15 Å from the U atom, that is, far enough to remain uncomplexed. The characteristics of the simulated systems are summarized in Table 4. Equilibration started with 2000 steps of steepest descent energy minimization, followed by 250 ps with fixed solutes ("BELLY" option in AMBER) at constant volume, and by 250 ps of constant volume without constraints, followed by 500 ps at a constant pressure of 1 atm coupling the system to a barostat with a relaxation time of 0.2 ps. Then MD was run for 5 ns in the (NVT) ensemble at 400 K.

The MD trajectories were saved every 1 ps and analyzed as in ref 13 with the MDS and DRAW software. The average structure of the solvent around $UO_2^{2+}$ was characterized by the radial distribution functions (RDFs) during the last 0.2 ns. The average coordination number (CN) of the solvent anions (O and N atoms of $Tf_2N^-$) and cations ($N_{butyl}$ and $H_{ring}$ atoms of $C_4mim^+$) were calculated up to a cutoff distance of the first peak of the RDF. Insights into energy features were obtained by group component analysis, using a 12 Å cutoff distance and PME correction for the electrostatics. The total potential energy of the system in solution was decomposed as $E_{tot} = E_{COMP} + E_{COMP\text{-}IL} + E_{ILIL}$ where $E_{COMP}$ is the internal energy of the complex (from QM optimized structures), $E_{COMP\text{-}IL}$ is the complex/solvent interaction energy ("solvation energy"), and $E_{ILIL}$ corresponds to the solvent/solvent interactions.

**Quantum Mechanical Calculations.** Selected complexes were optimized with the Gaussian03 software[37] at the HF and DFT (B3LYP) levels of theory. For uranium, we used the relativistic large core effective core potential (ECP) of the Los Alamos group with 78 electrons in the core and a [3s,3p,2d,2f] contracted valence basis set.[37] The Cl, N, O atoms were described with a 6-31+G* basis set.

## Experimental Results

**Uranyl Speciation As a Function of Nitrate Concentration.** We first analyzed as a reference an $UO_2(Tf_2N)_2$ solution in $C_4mimTf_2N$ in the absence of nitrates (sample A). After dissolution of the uranyl salt, EXAFS shows that the uranyl equatorial shell is composed of an average of five oxygen atoms at 2.43 Å. The small peak visible on the FT at $R + \Delta \sim 3.4$ Å could be attributed to ∼3 sulfur atoms at 3.62 Å, arising from the $CF_3SO_2$ groups of $Tf_2N^-$.

Figure 1 displays the UV−vis spectra of $UO_2(Tf_2N)_2$ and $UO_2(CF_3SO_3)_2$ solutions in $C_4mimTf_2N$, as a function of the

(24) Newville, M. *J. Synchrotron Radiat*. **2001**, *8*, 322.
(25) Newville, M.; Ravel, B.; Haskel, D.; Rehr, J. J.; Stern, A.; Yacoby, Y. *Phys. B* **1995**, *208−209*, 154.
(26) Ankudinov, A.; Rehr, J. J. *Phys. Rev. B* **2000**, *62*(4), 2437.
(27) Thuery, P.; Nierlich, M.; Keller, N.; Lance, M.; Vigner, J.-D. *Acta Crystallogr., Sect. C* **1995**, *51*, 1300.
(28) Watkin, D. J.; Denning, R. G.; Prout, K. *Acta Crystallogr., Sect. C* **1991**, *47*, 2517.
(29) Shuvalov, R. R.; Burns, P. C. *Acta Crystallogr., Sect. C* **2003**, *59*, 71.
(30) Case, D. A.; Pearlman, D. A.; Caldwell, J. W.; Cheatham III, T. E.; Wang, J.; Ross, W. S.; Simmerling, C. L.; Darden, T. A.; Merz, K. M.; Stanton, R. V.; Cheng, A. L.; Vincent, J. J.; Crowley, M.; Tsui, V.; Gohlke, H.; Radmer, R. J.; Duan, Y.; Pitera, J.; Massova, I.; Seibel, G. L.; Singh, U. C.; Weiner, P. K.; Kollman, P. A. *AMBER7*; University of California: San Francisco, CA, 2002.
(31) de Andrade, J.; Böes, E. S.; Stassen, H. *J. Phys. Chem. B* **2002**, *106*, 3546–3548.
(32) Canongia-Lopes, J. N.; Padua, A. A. H. *J. Phys. Chem. B* **2004**, *108*, 16893–16898.
(33) Guilbaud, P.; Wipff, G. *J. Mol. Struct. THEOCHEM* **1996**, *366*, 55–63.
(34) Baaden, M.; Berny, F.; Madic, C.; Wipff, G. *J. Phys. Chem. A* **2000**, *104*, 7659–7671.
(35) Sieffert, N.; Wipff, G. *J. Phys. Chem. B* **2006**, *110*, 13076–13085.
(36) Tokuda, H.; Hayamizu, K.; Ishii, K.; Susan, M. A. B. H.; Watanabe, M. *J. Phys. Chem. B* **2004**, *108*, 16593–16600.
(37) Ortiz, V.; Hay, P. J.; Martin, R. L. *J. Am. Chem. Soc.* **1992**, *114*, 2736.

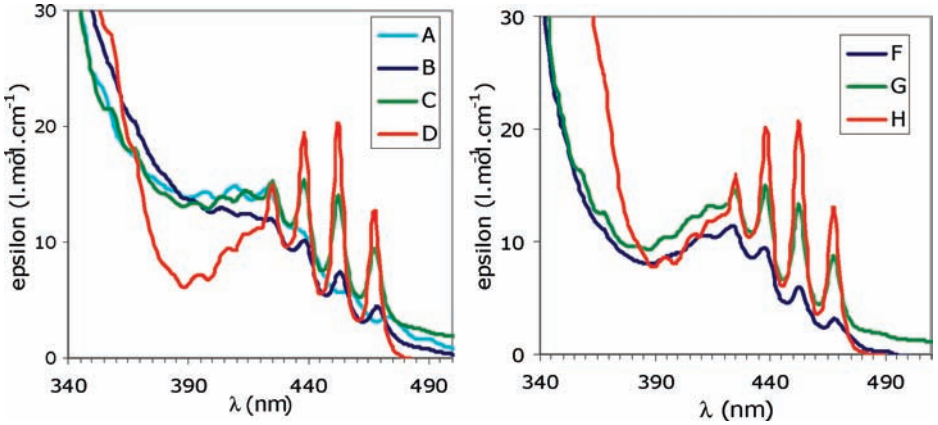


**Figure 1.** Influence of nitrates concentration on UV−vis spectra of a uranyl solution in $C_4mimTf_2N$ (see samples ID in Table 1). Left: solution of $UO_2(Tf_2N)_2$, spectrum A from ref 13. Right: solution of $UO_2(CF_3SO_3)_2$.

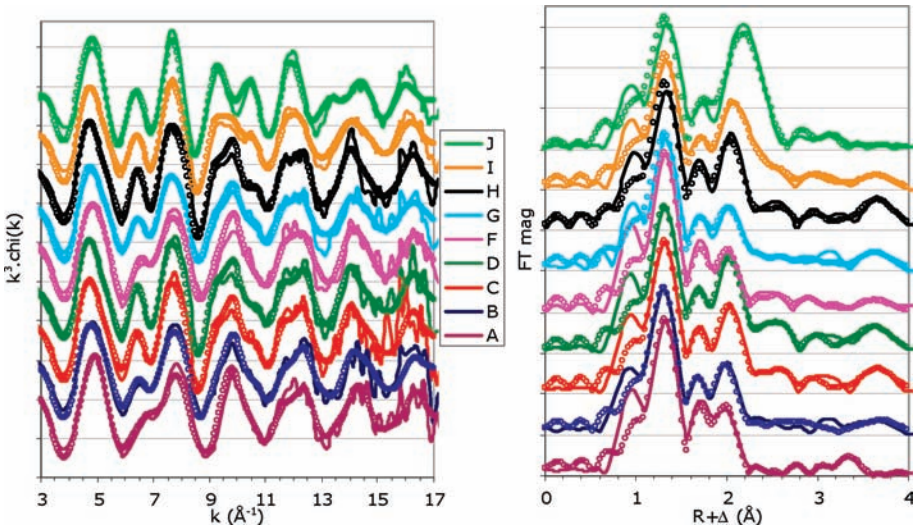


**Figure 2.** EXAFS spectra and their corresponding Fourier transform of uranyl samples described in Table 1. For the sake of clarity, spectra were shifted along the *y*-axis.

nitrate concentration for $[NO_3^-]/[UO_2^{2+}]$ ratio from 0 to 3 (samples A−H). For both salts, addition of nitrates entails the appearance of four intense bands at 425, 438, 452, and 467 nm, whose intensity increases with the nitrate concentration. Those bands are typical of uranyl-nitrato-complexes,[38] as observed in organic solvents[14,39] and in ILs.[13,14,21] Increased nitrate coordination is related to an increased absorbance of the four intense bands.[39] No change is observed as a function of the uranyl counterions ($Tf_2N^-$ or $CF_3SO_3^-$), indicating that in both cases nitrates are stronger ligands than $Tf_2N^-$ or triflates.

EXAFS spectra of the same samples are displayed in Figure 2, and fit results are given in Table 3. Addition of nitrates to a $UO_2(Tf_2N)_2$ or $UO_2(CF_3SO_3)_2$ solution entails strong changes on the EXAFS spectra, in particular in the 5−9 $Å^{-1}$ region. The corresponding Fourier transforms show changes in the equatorial shell in the region between $R + \Delta \sim 1.5$ and 2.2 Å while new peaks centered at $R + \Delta \sim 2.6$ and $R + \Delta \sim 3.8$ Å appear. The latter are the signature of a nitrate complexation to uranyl in a bidentate fashion. The peak at $R + \Delta \sim 2.6$ Å is characteristic of the nitrogen shell while the peak at $R + \Delta \sim 3.8$ Å arises from the distal oxygen atoms and is related with the multiple scattering of $U-N-O_{dist}$ atoms at the nitrate groups. Fits of these spectra show that at the different studied $[NO_3^-]/[UO_2^{2+}]$ ratio (from 1 to 3), the nitrate ions added in solution are totally complexed to uranyl, that is, no free nitrates are present in solution. Complexation of nitrate groups to uranyl results in a lengthening of $U-O_{equatorial}$ distances (from 2.43 to 2.48 Å) and an increase of the total equatorial oxygen number. The final complex formed is $UO_2(NO_3)_3^-$ whose structural parameters are identical to those obtained previously for a $UO_2(Tf_2N)_2$ solution where nitrates were added in excess over uranyl (ratio 4, sample E).[21] They are also similar to those obtained for dried $C_4mimTf_2N$ solution of $UO_2(NO_3)_2 \cdot 6H_2O$ + TBA-$NO_3$ where $[NO_3^-]/[UO_2^{2+}] = 4$.[14] The present study thus confirms that the $UO_2(NO_3)_3^-$ complex becomes completely dominating when $[NO_3^-]/[UO_2^{2+}] \geq 3$.

As for UV−vis spectroscopy, no difference between $UO_2(Tf_2N)_2$ and $UO_2(CF_3SO_3)_2$ solutions is visible by EXAFS.

**Competition between Two Strong Ligands, Nitrate and Chloride.** Our previous work[13] has shown that after dissolution of uranyl nitrate in $C_4mimTf_2N$, two nitrate ions, on the average, remain in the first uranyl coordination sphere, bound in a bidentate fashion, either as $UO_2(NO_3)_2$ or as a mixture of nitrato-species ($UO_2(NO_3)^+$, $UO_2(NO_3)_2$, and $UO_2(NO_3)_3^-$) originated by $UO_2(NO_3)_2$ dismutation.[40] After addition of chlorides

(38) Görller-Wallrand, C.; De Jaegere, S. *J. Chim Phys* **1972**, *4*, 726.
(39) Ikeda, A.; Hennig, C.; Rossberg, A.; Tsushima, S.; Scheinost, A. C.; Bernhard, G. *Anal. Chem.* **2008**, *80*, 1102.
(40) Rabinowitch, E.; Belford, R. L., *Spectroscopy and photochemistry of uranyl compounds*; Pergamon Press: Elmsford, NY, 1964.

**Table 3.** Fit Results for Uranyl Solutions in $C_4mimTf_2N$, Described in Table 1[a]

| sample ID | shell | CN | $R$ (Å) | $\sigma^2$ (Å$^2$) | $E_0$ (eV) | $R_{factor}$ |
|---|---|---|---|---|---|---|
| A | $O_{axial}$ | 2[b] | 1.75(1) | 0.002(1) | | |
| | $O_{equatorial}$ | 5.1(9) | 2.43(1) | 0.008(2) | −8.1 | 0.01 |
| | S | 2.7(6) | 3.62(1) | 0.005(1) | | |
| B | $O_{axial}$ | 2[b] | 1.75(1) | 0.002(1) | | |
| | $O_{equatorial}$ | 4.7(8) | 2.45(1) | 0.008(2) | −9 | 0.02 |
| | N | 0.9(4) | 2.92(2) | 0.003(1) | | |
| | $O_{distal}$ | 0.9[c] | 4.16(2) | 0.003(1) | | |
| C | $O_{axial}$ | 2[b] | 1.76(1) | 0.002(1) | | |
| | $O_{equatorial}$ | 5.9(8) | 2.47(1) | 0.008(2) | −10 | 0.02 |
| | N | 2.3(6) | 2.92(2) | 0.003(1) | | |
| | $O_{distal}$ | 2.3[c] | 4.16(2) | 0.006(1) | | |
| D | $O_{axial}$ | 2[b] | 1.76(1) | 0.002(1) | | |
| | $O_{equatorial}$ | 5.5(4) | 2.48(1) | 0.007(2) | −9.7 | 0.02 |
| | N | 3.0(3) | 2.92(1) | 0.004(1) | | |
| | $O_{distal}$ | 3.0[c] | 4.15(1) | 0.006(1) | | |
| E (from ref 21) | $O_{axial}$ | 2[b] | 1.76(1) | 0.002(1) | | |
| | $O_{equatorial}$ | 6[b] | 2.49(1) | 0.008(2) | −8.5 | 0.01 |
| | N | 3[b] | 2.93(1) | 0.005(1) | | |
| | $O_{distal}$ | 3[b] | 4.18(2) | 0.004(1) | | |
| F | $O_{axial}$ | 2[b] | 1.76(1) | 0.002(1) | | |
| | $O_{equatorial}$ | 4.4(5) | 2.44(1) | 0.009(2) | −9.1 | 0.02 |
| | N | 1.1(5) | 2.92(2) | 0.003(1) | | |
| | $O_{distal}$ | 1.1[c] | 4.15(2) | 0.005(1) | | |
| G | $O_{axial}$ | 2[b] | 1.76(1) | 0.002(1) | | |
| | $O_{equatorial}$ | 5.9(9) | 2.48(1) | 0.011(3) | −8.4 | 0.03 |
| | N | 1.8(6) | 2.94(2) | 0.005(1) | | |
| | $O_{distal}$ | 1.8[c] | 4.16(2) | 0.005(1) | | |
| H | $O_{axial}$ | 2[b] | 1.77(1) | 0.002(1) | | |
| | $O_{equatorial}$ | 6.0(6) | 2.49(1) | 0.008(2) | −8.1 | 0.03 |
| | N | 2.8(7) | 2.92(2) | 0.005(1) | | |
| | $O_{distal}$ | 2.8[c] | 4.16(2) | 0.005(1) | | |
| I | $O_{axial}$ | 2[b] | 1.77(1) | 0.002(1) | | |
| | $O_{equatorial}$ | 3.8(7) | 2.51(1) | 0.008(2) | | |
| | Cl | 1.0(3) | 2.67(2) | 0.005[b] | −7.2 | 0.02 |
| | N | 1.9(5) | 2.93(1) | 0.004(1) | | |
| | $O_{distal}$ | 1.9[c] | 4.18(2) | 0.007(2) | | |
| J | $O_{axial}$ | 2[b] | 1.77(1) | 0.003(1) | | |
| | Cl | 3.5(3) | 2.69(1) | 0.005[b] | −1.9 | 0.04 |

[a] CN is the coordination number, $R$ the interatomic distance, $\sigma^2$ the Debye-Waller factor, and $R_{factor}$ the goodness of the fit as defined in ref 25. [b] Fixed parameters. [c] Linked parameters.

at a [Cl]/[U] ratio of 4 in this uranyl nitrate solution, it was not clear whether chloride ions totally complexed to uranyl to form $UO_2Cl_4^{2-}$, in spite of their higher concentration compared to the nitrate one. To further investigate the competition between nitrate and chloride ions, we have analyzed eight new samples containing different amounts of nitrates and chlorides, added either as $C_4$mim-salts or TBA-salts (see sample composition in Table 2). Samples I and J correspond to solutions of uranyl nitrate in which chlorides were added as TBA-Cl to obtain a $[Cl^-]/[UO_2^{2+}]$ ratio of 2 (sample I) and 6 (sample J), that is, a $[Cl^-]/[NO_3^-]$ ratio of 1 (sample I) and 3 (sample J), respectively. On the Fourier transforms of the EXAFS spectra (Figure 2), addition of chlorides entails the appearance of a marked peak at $R + \Delta \sim 2.2$ Å, indicating chloride complexation to uranyl. The sample I spectrum also exhibits peaks at $R + \Delta \sim 2.6$ Å and $R + \Delta \sim 3.8$ Å, arising from a bidentate coordination of nitrates. These peaks are not seen in sample J. In sample I, where the chloride and nitrate concentrations are the same, fit of the EXAFS shows that the 2 nitrates on average remain in the uranyl coordination sphere, which is completed by ~1 $Cl^-$, leading to a total equatorial CN of 5. It was not possible to obtain a reliable fit of the data assuming a higher coordination of chlorides, that is, 2 Cl, even assuming a total equatorial CN of 5 or 6. For sample J, where chlorides are in excess over nitrates (1:2:6 $U/NO_3/Cl$ ratio), EXAFS fits show that uranyl is coordinated by ~3.5 Cl at U−Cl distances

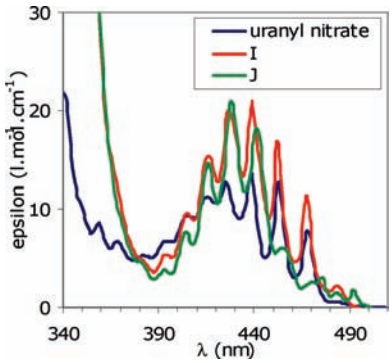


**Figure 3.** UV−vis spectra of uranyl nitrate solution in $C_4mimTf_2N$, as a function of the chloride concentration. Data for the "uranyl nitrate" sample is from ref 13.

of 2.69 Å, as previously obtained with a 1:2:4 $U/NO_3/Cl$ ratio.[13] No better fits could be obtained by adding an oxygen equatorial shell (from monodentate $Tf_2N^-$ or nitrate ions) or shells involving bidentate or monodentate nitrates (nitrogen shell and distal oxygen shell). At this stage, EXAFS results on sample J are thus best interpreted considering that the uranyl complex in solution is dominated by $UO_2Cl_4^{2-}$.

The UV−vis spectra of samples I and J are displayed in Figure 3. The spectrum of a pure uranyl nitrate solution in $C_4mimTf_2N$, also plotted as a reference (see ref 13), exhibits four intense bands at 425, 437, 453, and 468 nm, typical of a nitrato-uranyl complex. Addition of chlorides at a $[Cl^-]/[NO_3^-]$ ratio of 1 (sample I) entails a global increase of the molar absorbance. Upon addition of an excess of chloride (sample J), three intense bands at 415, 428, and 441 nm are still visible, but bands at 453 and 467 nm have disappeared. The UV−vis spectrum of sample J differs significantly from the typical spectrum of $UO_2Cl_4^{2-}$,[13,41,42] expected from the EXAFS results: the absorbance of sample J is much higher than that of the $UO_2Cl_4^{2-}$ species, and we furthermore note the absence of fine-structures arising from the $D_{4h}$ symmetry of the $UO_2Cl_4^{2-}$ complex, suggesting that the complex is in fact less symmetrical.

To further investigate this unusual feature in the UV−vis spectrum, we studied the influence of the nitrate concentration on the chloride/nitrate competition (Figure 4). We first compared results obtained by using either tetrabutylammonium or imidazolium salts of chloride and nitrate (samples K, L, M, N, O, defined in Table 2). As expected, dissolving a 4-fold excess of $C_4mimCl$ in a $UO_2(Tf_2N)_2$ solution results in a UV−vis spectrum identical to the one obtained using TBA-Cl (samples L vs K), indicating the presence of $UO_2Cl_4^{2-}$ species with either $C_4min^+$ or $TBA^+$ counterions. Addition of nitrates to this solution, either as $TBA\text{-}NO_3$ or $C_4mimNO_3$, at a $[NO_3^-]/[UO_2^{2+}]$ ratio ranging from 3 to 12, entails drastic changes in the UV−vis spectra (samples M, N, O in Figure 4) whose shape and intensity become identical to the one of sample J. We thus observe neither clear evolution in the UV−vis spectra as a function of the nitrate versus chloride counterions nature nor as a function of the nitrate concentration. Even at highest nitrate concentration, the UV−vis spectra clearly differ from those of uranyl nitrate containing solutions without chlorides (see Figure 1).

We then compared solutions with the same $[UO_2^{2+}]/[NO_3^-]/[Cl^-]$ ratio of 1/2/6, but prepared in different ways: sample P has the same anionic composition as sample J but prepared in two steps. First, uranyl ions were introduced as $UO_2(Tf_2N)_2$ salt in $C_4mimTf_2N$, and a 2-fold excess of $C_4mim\text{-}NO_3$ was added. The UV−vis spectrum of this solution (not shown) is

(41) Sornein, M.-O.; Cannes, C.; Le Naour, C.; Lagarde, G.; Simoni, E.; Berthet, J.-C. *Inorg. Chem.* **2006**, *45*, 10419.
(42) Görller-Wallrand, C.; De Houwer, S.; Fluyt, L.; Binnemans, K. *Phys. Chem. Chem. Phys.* **2004**, *6*, 3292.

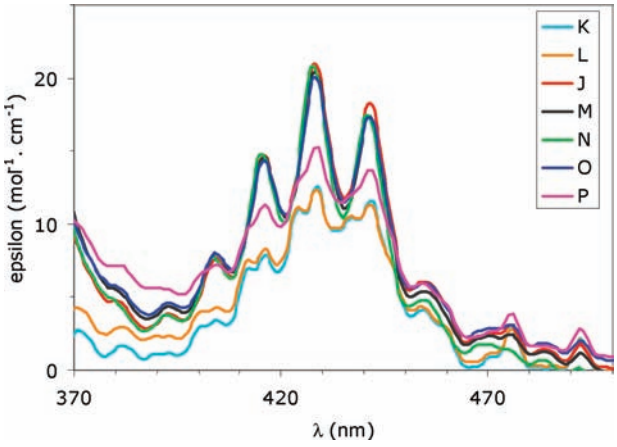


**Figure 4.** UV−vis spectra of $UO_2(Tf_2N)_2$ solution in $C_4mimTf_2N$ as a function of the chloride and nitrate concentration.

similar to the one obtained for $UO_2(NO_3)_2$ dissolved in $C_4mimTf_2N$.[13] We then added a 6-fold excess of $C_4mimCl$. The resulting UV−vis spectrum, displayed in Figure 4, is to be compared to the one of sample J, prepared by dissolving the $UO_2(NO_3)_2$ salt in $C_4mimTf_2N$ and adding of a 6-fold excess of chloride. Contrary to expectations, UV−vis spectra of samples P and J are quite different: the former exhibits a lower intensity and a slightly different shape, with the appearance of shoulders at 412, 424, and 437 nm. Those bands are also observed in the UV−vis spectrum of $UO_2Cl_4^{2-}$. The UV−vis spectrum of sample P thus displays intermediate features between those observed for sample J and for $UO_2Cl_4^{2-}$.

## Solvation of Uranyl Complexes: MD Simulation Results

MD simulations focused on the I and J solutions, with the main aim to compare the solvation and energy features of several types of uranyl complexes, and to analyze the apparent conflicting EXAFS and UV−vis results for the J solution. We thus simulated complexes formed upon addition of $n$ $Cl^-$ anions ($n$ = 2 and 6) to $C_4mimTf_2N$ solution of $UO_2(NO_3)_2$, and compared systems of identical compositions, where the $UO_2^{2+}/NO_3^-/Cl^-$ ratio is respectively 1/2/2 and 1/2/6 (see Table 4), as in I and J samples, respectively. They thus all contain 2 $NO_3^-$ species, whereas the $Cl^-$ concentration is "low" (1/2/2 ratio) or "high" (1/2/6 ratio). All complexes retained their ligands during the 5 ns of dynamics, without capturing additional free $Cl^-$ or $NO_3^-$ species. However, in some cases, $Tf_2N^-$ anions of the IL completed the uranyl solvation shell. In the following, we describe typical solvation features of the complexes. Energy features are discussed in the next section.

**Solvation of $UO_2(NO_3)_2$, $UO_2Cl(NO_3)_2^-$, $UO_2Cl_2(NO_3)^-$, and $UO_2Cl_2(NO_3)_2^{2-}$ (*cis* or *trans*) in $C_4mimTf_2N$ ILs ("Low" $Cl^-$ Concentration).** Typical snapshots of the different complexes with their first and second solvation shells and solvent RDFs around the U atom are given in Figure 5. They show that in all complexes $UO_2^{2+}$ is surrounded in the equatorial plane by anions, either initially complexed ($Cl^-$ and $NO_3^-$) or stemming from the solvent ($Tf_2N^-$). The U atom of $UO_2(NO_3)_2$ further coordinates 2 monodentate $Tf_2N^-$ anions via their O atom. The $Tf_2N^-$ coordination is dynamic as the coordinated oxygen atoms exchange during the simulation, leading to a total coordination number (CN) of 6, with average U−O distances of about 2.55 Å.[43] In the more hindered $UO_2Cl(NO_3)_2^-$ and $UO_2Cl_2(NO_3)^-$ complexes, uranyl likewise coordinates, on average, one monodentate $Tf_2N^-$ anion in its equatorial plane, at average U−O distances of about 2.61 Å and 2.57 Å, respectively. For the 6-coordinated $UO_2Cl_2(NO_3)_2^{2-}$(*cis* or *trans*) complexes, the coordination sphere remains identical in the IL as in the gas phase. The U−Cl distances are 2.56 Å in the studied chloro-complexes. All complexes, formally anionic, are surrounded by a second solvation shell, comprising about 5 $C_4mim^+$ cations up to 7 Å.

**Table 4.** Characteristics of the Simulated Systems

| solute | solvent components | box size (Å$^3$) |
|---|---|---|
| Solutions with 1/2/2 U/Cl/$NO_3$ Ratio | | |
| $UO_2(NO_3)_2$, 2 $Cl^-$ | 200 $C_4mim^+$ + 198 $Tf_2N^-$ | 45.4[3] |
| $UO_2Cl(NO_3)_2$, $Cl^-$ | 200 $C_4mim^+$ + 198 $Tf_2N^-$ | 45.3[3] |
| $UO_2Cl_2(NO_3)$, $NO_3^-$ | 200 $C_4mim^+$ + 198 $Tf_2N^-$ | 45.3[3] |
| $UO_2Cl_2(NO_3)_2^{2-}$ (*cis*) | 200 $C_4mim^+$ + 198 $Tf_2N^-$ | 45.3[3] |
| $UO_2Cl_2(NO_3)_2^{2-}$ (*trans*) | 200 $C_4mim^+$ + 198 $Tf_2N^-$ | 45.3[3] |
| Solutions with 1/6/2 U/Cl/$NO_3$ Ratio | | |
| $UO_2Cl_3(NO_3)^{2-}$, 3 $Cl^-$ + $NO_3^-$ | 200 $C_4mim^+$ + 194 $PF_6^-$ | 45.2[3] |
| $UO_2Cl_4^{2-}$, 2 $Cl^-$ + 2 $NO_3^-$ | 200 $C_4mim^+$ + 194 $PF_6^-$ | 45.1[3] |

**Solvation of $UO_2Cl_2(NO_3)_2^{2-}$, $UO_2Cl_3(NO_3)^{2-}$, and $UO_2Cl_4^{2-}$ in $C_4mimTf_2N$ IL ("High" $Cl^-$ Concentration).** During the simulation of the $UO_2Cl_2(NO_3)_2^{2-}$, $UO_2Cl_3(NO_3)^{2-}$, and $UO_2Cl_4^{2-}$ complexes, no solvent anion coordinated to the U atom. These complexes thus retained the same CN in solution as in the gas phase: 6, 5, and 4, respectively. Like in the less concentrated $Cl^-$ solution, the equatorial anionic shell of uranyl is surrounded by a cationic shell, of about 5 $C_4mim^+$ cations within 7 Å. From the cumulated views in Figure 6 one sees that the latter are generally oriented with their imidazolium ring protons H-bonded toward $Cl^-$ ligands while their alkyl chains point away. This is particularly visible for $UO_2Cl_4^{2-}$, while for the $UO_2Cl_2(NO_3)_2^{2-}$ and $UO_2(NO_3)_2$ complexes, imidazoliums are more disordered, hinting for weaker interactions between the uranyl ligands and $C_4mim^+$ cations.

**Insights into the $Cl^-$ versus $NO_3^-$ Coordination to Uranyl in the Gas Phase and in Solution.** In the gas phase, the competition between $Cl^-$ and $NO_3^-$ ligands was analyzed via reactions (1) to (11), defined in Table 6, and the corresponding energies obtained at the HF and DFT levels of theory. Reactions (1) to (4) correspond to the substitution of all $NO_3^-$ by $Cl^-$ ligands in complexes of $UO_2X_n^{2-n}$ type ($n$ = 1 to 4), reactions (5) to (7) correspond to $Cl^-$ addition to $UO_2(NO_3)_2$ or $UO_2(NO_3)_2Cl^-$ complexes, and in reactions (8) to (11) a $NO_3^-$ ligand is replaced by a $Cl^-$ ligand in mixed chloro-nitrato complexes. The energies $\Delta E_1-\Delta E_{11}$ obtained at the HF and DFT levels of theory generally yield similar qualitative conclusions, but may differ at the quantitative level (by up to ca. 10 kcal/mol for reactions (1) to (4)). In the following, we use DFT results that are in principle more satisfactory because they better account for correlation effects. Both computation methods

(43) Because the force field parameters have not been optimized on structural features of the uranyl complexes, these distances cannot be directly compared with those obtained, that is, by EXAFS. They are in fact about 0.08 Å longer.

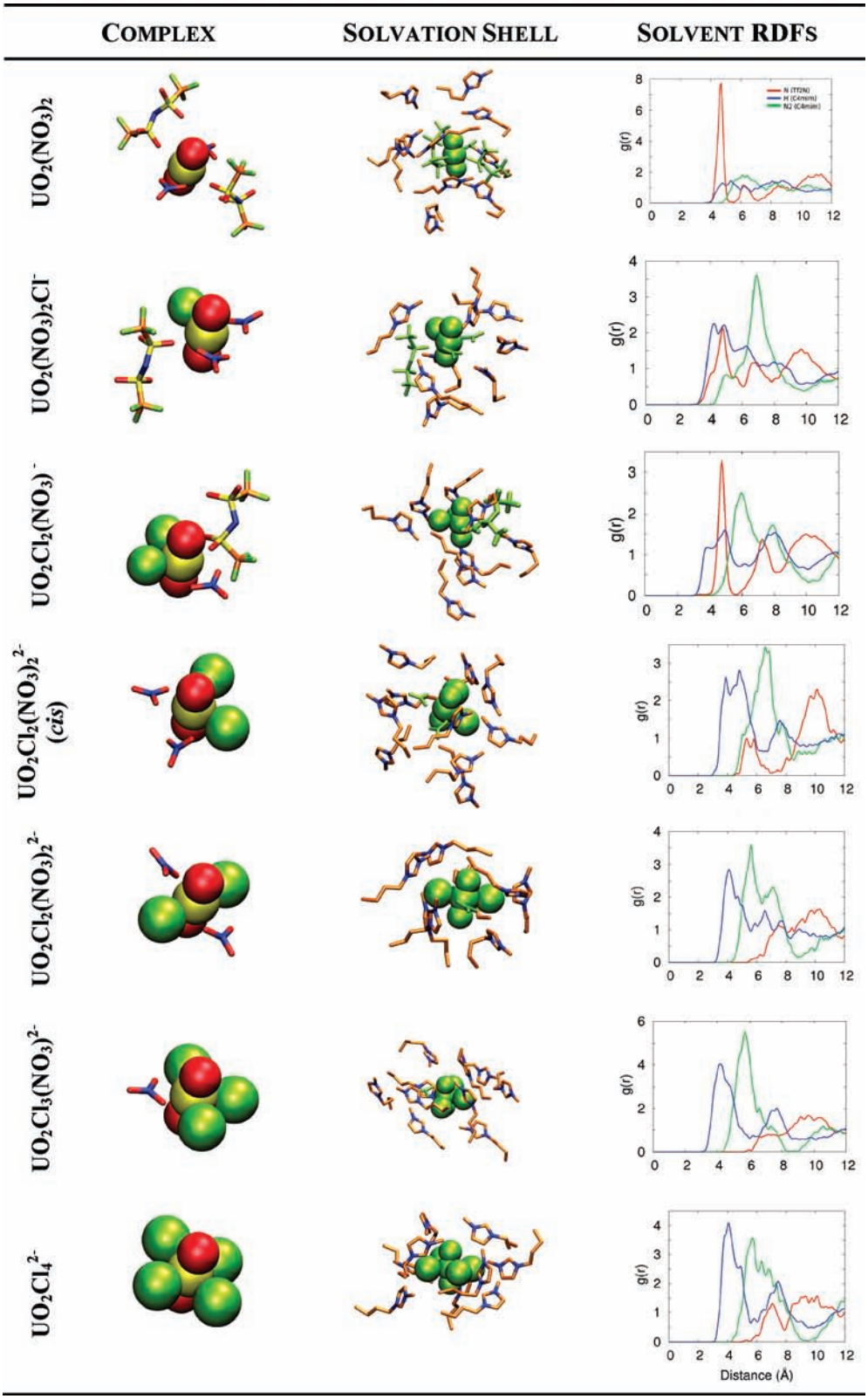


**Figure 5.** $UO_2Cl_n(NO_3)_m^{2-m-n}$ complexes simulated in $C_4mimTf_2N$. From left to right: Snapshots of the first shell (anions), of the first and second solvation shell (anions + $C_4mim^+$) of uranyl, and U···IL RDFs ($N_{Tf2N}$ in red, $H_{C4mim\text{-}ring}$ in blue, $N_{C4mim}$ in green).

show that the $Cl^-$ versus $NO_3^-$ preference depends on the saturation of the complex and on the nature of its other ligands. In most cases, $NO_3^-$ coordinates bidentate to uranyl (there is one exception with $UO_2(NO_3)_4^{2-}$ of $D_{2h}$ symmetry, where two nitrates are monodentate, as in the solid state structure),[44] yielding coordination numbers CN ranging from 2 to 6, depending on the complex. Reactions

(44) Bradley, A. E.; Hardacre, C.; Nieuwenhuyzen, M.; Pitner, W. R.; Sanders, D.; Seddon, K. R.; Thied, R. C. *Inorg. Chem.* **2004**, *43*(8), 2503.

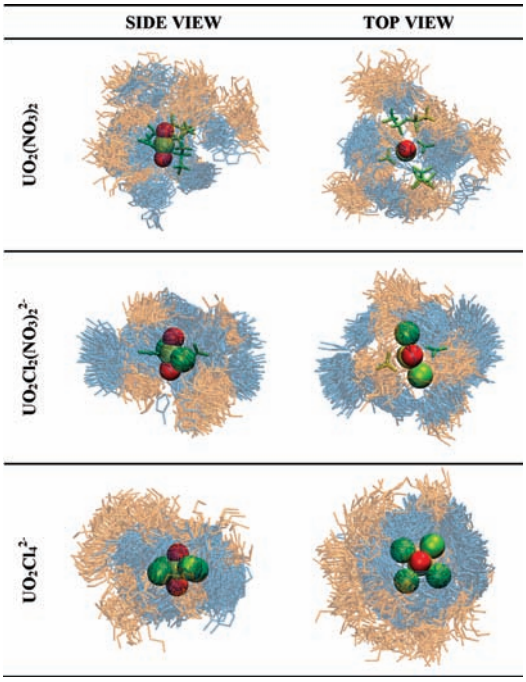


**Figure 6.** Cumulated views of the $C_4mim^+$ cations around the $UO_2(NO_3)_2$, $UO_2Cl_2(NO_3)_2^{2-}$, and $UO_2Cl_4^{2-}$ complexes, colored with their imidazolium ring (blue) and butyl chain (orange). Snapshots every 5 ps over the last 500 ps of dynamics.

**Table 5.** Characteristics of the $C_4mimTf_2N$ Solvent RDFs around the Uranyl Complexes[a]

| solute | $N_{Tf2N}$ | $N2_{C4mim}$ | $H_{C4mim}$ |
|---|---|---|---|
| $UO_2(NO_3)_2$, 2 $Cl^-$ | 2 | 3.9 | 6.5 |
| | (4.7 ; 5.2) | (6.1 ; 7.7) | (5.3 ; 6.7) |
| $UO_2Cl(NO_3)_2^-$, $Cl^-$ | 1.6 | 9.2 | 6.1 |
| | (4.8 ; 6.1) | (6.9 ; 9.8) | (4.3 ; 5.5) |
| $UO_2Cl_2(NO_3)^-$, $NO_3^-$ | 1.1 | 3.9 | 5 |
| | (4.7 ; 5.6) | (5.9 ; 7.2) | (4.9 ; 5.9) |
| $UO_2Cl_2(NO_3)_2^{2-}$ (*cis*) | 1 | 6.4 | 10.5 |
| | (5.3 ; 7.0) | (6.6 ; 7.5) | (4.8 ; 6.5) |
| $UO_2Cl_2(NO_3)_2^{2-}$ (*trans*) | 2 | 3.4 | 6.6 |
| | (7.5 ; 8.1) | (5.6 ; 6.4) | (4.1 ; 5.6) |
| $UO_2Cl_3(NO_3)^{2-}$ | 1.5 | 5.5 | 9.8 |
| | (7.1 ; 7.8) | (5.7 ; 6.5) | (5.2 ; 6.0) |
| $UO_2Cl_4^{2-}$ | 2 | 4.3 | 8.7 |
| | (7.0 ; 7.9) | (5.7 ; 6.6) | (4.1 ; 5.6) |

[a] Coordination number (first line) obtained by integration of the first peak whose maximum and integration distance are indicated in parentheses (second line; Å).

**Table 6.** Reaction Energies in the Gas Phase (kcal/mol) from HF and DFT Calculations

| | HF | B3LYP |
|---|---|---|
| (1) $UO_2NO_3^+ + Cl^- \rightarrow UO_2Cl^+ + NO_3^-$ | 8.9 | 0.8 |
| (2) $UO_2(NO_3)_2 + 2Cl^- \rightarrow UO_2Cl_2 + 2NO_3^-$ | 14.8 | 3.0 |
| (3) $UO_2(NO_3)_3^- + 3Cl^- \rightarrow UO_2Cl_3^- + 3NO_3^-$ | 11.6 | 2.1 |
| (4) $UO_2(NO_3)_4^{2-} + 4Cl^- \rightarrow UO_2Cl_4^{2-} + 4NO_3^-$ | 2.7 | −11.0 |
| (5) $UO_2(NO_3)_2 + Cl^- \rightarrow UO_2Cl(NO_3)_2^-$ | −72.4 | −70.6 |
| (6) $UO_2Cl(NO_3)_2^- + Cl^- \rightarrow UO_2Cl_2(NO_3)_2^{2-}$ (*cis*) | 34.6 | 33.5 |
| (7) $UO_2Cl(NO_3)_2^- + Cl^- \rightarrow UO_2Cl_2(NO_3)_2^{2-}$(*trans*) | 40.7 | 37.8 |
| (8) $UO_2Cl(NO_3)_2^- + Cl^- \rightarrow UO_2Cl_2(NO_3)^- + NO_3^-$ | 3.8 | 0.3 |
| (9) $UO_2Cl_2(NO_3)_2^{2-}$ (*cis*) + $Cl^- \rightarrow UO_2Cl_3(NO_3)^{2-} + NO_3^-$ | 1.7 | −1.5 |
| (10) $UO_2Cl_2(NO_3)_2^{2-}$ (*trans*) + $Cl^- \rightarrow UO_2Cl_3(NO_3)^{2-} + NO_3^-$ | −4.4 | −5.8 |
| (11) $UO_2Cl_3(NO_3)^{2-} + Cl^- \rightarrow UO_2Cl_4^{2-} + NO_3^-$ | −0.8 | −2.8 |

(1) to (3) indicate that, intrinsically, nitrates are preferred over chlorides in one- to three- coordinated complexes. In the 4-coordinated complex, chlorides become preferred (CN = 4), because of the high interligand repulsion in the $UO_2(NO_3)_4^{2-}$ complex (CN = 6).

As expected, chloride addition to the dinitrato complex is clearly favored when uranyl is 4- coordinated and unsatured ($\Delta E_5 = -70$ kcal/mol), but strongly disfavored when it is 5-coordinated ($\Delta E_6$ and $\Delta E_7$ are higher than 33 kcal/mol). The effect of substituting $NO_3^-$ by $Cl^-$ in saturated mixed chloro-nitrato complexes is less clear-cut ($\Delta E_8$ to $\Delta E_{11}$ range from 0.3 to −5.8 kcal/mol). The most negative energies correspond to the formation of the $UO_2Cl_3(NO_3)^{2-}$ complex from $UO_2Cl_2(NO_3)_2^{2-}$ ($\Delta E_{10} = -5.8$ kcal/mol), and to the formation of $UO_2Cl_4^{2-}$ from $UO_2Cl_3(NO_3)^{2-}$ ($\Delta E_{11} = -2.8$ kcal/mol), likely because of the release of interligand repulsions. On the other hand, there is almost no preference for $UO_2Cl_2(NO_3)^-$, compared to $UO_2Cl(NO_3)_2^-$ ($\Delta E_8 = 0.3$ kcal/mol), presumably because of compensation between binding strength (favors $NO_3^-$) and steric hindrance (favors $Cl^-$).

In IL solution, the stability of the complexes depends on their intrinsic structure and energetics (sometimes different in solution compared to the gas phase), their solvation (including co-complexation of $Tf_2N^-$ IL anions), on the solvation of the free ions, and on the internal energy of the solvent. Furthermore, the thermodynamics of solvation involves enthalpy and entropy components, whose changes might be obtained in principle by free energy simulations (see, for example, ref 45). This is, however, a difficult and computer consuming task because of sampling issues and force field limitations, and is beyond the scope of this paper. We thus decided to analyze important energy components and their changes for model reactions that mimic experiments I and J on the $Cl^-/NO_3^-$ competition (see Table 7). Because simulations on free versus complexed chlorides have been carried out with identical numbers of solvent and solute molecules, one can indeed calculate the change $\Delta E_{COMP\text{-}IL}$ of interaction energies between the complex with its IL environment and the change $\Delta E_{ILIL}$ in internal energy of the liquid itself, including uncomplexed nitrates or chlorides in the IL group. The sum $\Delta E_{tot} = \Delta E_{COMP\text{-}IL} + \Delta E_{ILIL} + \Delta E_{COMP}$, where the energy change of the complex has been obtained by QM (DFT) calculations in the gas phase, thus accounts for important contributions of the solvation changes and intrinsic complex stabilities. Note that fluctuations on $E_{COMP\text{-}IL}$ and $E_{ILIL}$ are high (ca. 50 kcal/mol), calling for care in the analysis of $\Delta E_{tot}$. The results are presented in Table 7 for $Cl^-$ complexation reactions Ia and Ib and for ligand exchange reactions Ic, Ja, and Jb. As expected, $Cl^-$ complexation renders the complex more negatively charged, thus enhancing its solvation ($\Delta E_{COMP\text{-}IL} < 0$) and destabilizing the IL phase ($\Delta E_{ILIL} > 0$). The net balance for reaction Ia is close to zero, showing that there is no strong driving force to complex $Cl^-$ from the dinitrato complex in solution. This is consistent with the quasi-nul $\Delta E_{tot}$ energy of reaction Ic where $Cl^-$ displaces a $NO_3^-$ ligand from the $UO_2Cl(NO_3)_2^-$ complex.

Regarding reactions Ja and Jb that model experiment J with a $U/NO_3^-/Cl^-$ ratio of 1/2/6, the results are more

(45) Chaumont, A.; Wipff, G. *J. Phys. Chem. B* **2008**, *112*(38), 12014–12023.

**Table 7.** Reactions Energies (kcal/mol) "in $C_4$min $Tf_2N$ Solution"

| | $\Delta E_{COMP}$ [a] | $\Delta E_{COMP\text{-}IL}$ [b] | $\Delta E_{ILIL}$ [b] | $\Delta E$ [c] |
|---|---|---|---|---|
| Systems Corresponding to Experiment I (1: 2: 2 U/$NO_3$/Cl Ratio) | | | | |
| **Ia** $UO_2(NO_3)_2 + 2Cl^- \rightarrow UO_2Cl(NO_3)_2^- + Cl^-$ | (−71) [d] | −25 | 106 | (10) [d] |
| **Ib** $UO_2Cl(NO_3)_2^- + Cl^- \rightarrow UO_2Cl_2(NO_3)_2^{2-}$ | 38 | −208 | 201 | 40 |
| **Ic** $UO_2Cl(NO_3)_2^- + Cl^- \rightarrow UO_2Cl_2(NO_3)^- + NO_3^-$ | 1 | −5 | 7 | 3 |
| System Corresponding to Experiment J ( 1: 2: 6 U/$NO_3$/Cl Ratio) | | | | |
| **Ja** $UO_2Cl_2(NO_3)_2^{2-} + 4Cl^- \rightarrow UO_2Cl_3(NO_3)^{2-} + 3Cl^- + NO_3^-$ | −6 | −34 | −7 | −47 |
| **Jb** $UO_2Cl_3(NO_3)^{2-} + 3Cl^- \rightarrow UO_2Cl_4^{2-} + NO_3^- + 2Cl^-$ | −3 | 20 | 33 | 50 |

[a] $\Delta E_{COMP}$ obtained by QM gas phase optimizations at the DFT/B3LYP-6-31+G* level. [b] $\Delta E_{COMP\text{-}IL}$ and $\Delta E_{ILIL}$ obtained from MD simulation in solution, considering all uncomplexed ions as solvent. $Cl_{TCA}$ parameters for Cl. [c] $\Delta E = \Delta E_{COMP} + \Delta E_{COMP\text{-}IL} + \Delta E_{ILIL}$. [d] Note that in the IL solution, the nitrates of the $UO_2(NO_3)_2$ complex are not *trans* like in the gas phase, but *"cis"*, because of the coordination of 2 $Tf_2N^-$ solvent anions. As a result, the $\Delta E_{COMP}$ and $\Delta E$ energies should be lower, by about 10 kcal/mol (destabilization energy of the $UO_2(NO_3)_2$ moiety of $UO_2(NO_3)_2(Tf_2N)_2$, relative to the $UO_2(NO_3)_2$ complex; QM optimizations).

clear-cut. Formation of the mixed $UO_2Cl_3(NO_3)^{2-}$ complex from $UO_2Cl_2(NO_3)_2^{2-}$ is preferred by −47 kcal/mol (because of favorable changes in the $\Delta E_{COMP\text{-}IL}$, $\Delta E_{ILIL}$, and $\Delta E_{COMP}$ components), whereas the formation of the $UO_2Cl_4^{2-}$ complex is disfavored by 50 kcal/mol, because of solvation effects.

## Discussion

**Uranyl Speciation As a Function of Nitrate Concentration.** As a reference we have first characterized by EXAFS a $C_4$mim$Tf_2N$ solution in which uranyl was dissolved as $UO_2(Tf_2N)_2$ (sample A) where uranyl displays a typical equatorial sphere with five oxygen atoms at 2.43 Å. This is comparable to the equatorial shell obtained by dissolution of uranyl perchlorate or triflate in $C_4$mim$Tf_2N$.[13] By comparison, a CN of 6 was obtained by molecular dynamics calculation[13] of a solvated $UO_2^{2+}$ ion dissolved in $C_4$mim$Tf_2N$, while Bhatt et al.[46] got a CN of 4 by the EXAFS analysis after dissolution of the same salt in the tetra-alkylammonium IL $Me_3BuNTf_2N$. These authors also detected a sulfur shell at a U−S distance of 3.59 Å, close to the value of 3.62 Å we observe. To our knowledge there is no X-ray crystal structure of uranyl−$Tf_2N$ coordination reported so far, but structures are available for the triflate $CF_3SO_3^-$ which can be considered as analogue of $Tf_2N^-$, with typical U···$SO_3$ distances of 3.7−3.8 Å (monodentate), 3.2 Å (bidentate), and 3.6−3.7 Å (bridging).[47−50] Although it is difficult to safely conclude on the coordination mode of $Tf_2N^-$ in solution from a single U−S distance, we note that our observed U···S distance is consistent with monodentate and bridging coordinations but not with bidentate coordination. The preference for monodentate over bi- or tridentate binding mode is consistent with MD simulation results of $UO_2^{2+}$ in the $C_4$mim$Tf_2N$ solution where uranyl coordinates five $Tf_2N^-$ anions: three monodentate, one bidentate, and one exchanging between both modes.[13] In case of bridging U···OSO···U patterns, the U···U signature would occur at about 6.5 Å, which is too long to be observed on the EXAFS spectrum. For $Cl^-$ or $NO_3^-$ uranyl ligands, oligomeric complexes with bridging ligands would involve shorter U···U distances (ca. 4.3−4.8 Å).[51] The lack of a peak in this EXAFS region indicates that the corresponding complexes are most likely monomeric.

We have then studied $UO_2(Tf_2N)_2$ in $C_4$mim$Tf_2N$ solutions to which nitrates were added at different ratio. Like chlorides, nitrates are rather weak ligands of uranyl in water where a large concentration is required to form mono- and dinitrato complexes. They are, however, strong ligands in ILs and organic solvents. In $C_4$mim$Tf_2N$ solution, when 3 equiv or more of nitrates are added, the uranyl trinitrato complex is formed as shown by the structural parameters and UV−vis spectrum obtained, similar to those obtained in other organic media[38−40] or ILs.[14,21,52] While in sample A (i.e., without nitrates) we could detect a sulfur shell arising from the $Tf_2N$ group, this was not possible in the spectra of samples B and F (1 equiv of $NO_3$). This may be due to a lack of sensitivity of the technique and/or different coordination modes of $Tf_2N$ (e.g., monodentate vs bidentate). In samples C and G, where an average of 2 nitrates are coordinated to uranyl, the uncertainty on the CN determination by EXAFS ($CN_{eq}$ = 5.9 ± 1.2) does not allow to safely discriminate between a five- or six-fold coordination. Nevertheless, the U−$O_{eq}$ bond distances obtained, 2.47 and 2.48 Å respectively for samples C and G, support a six-fold equatorial coordination, consistent with the results obtained by Ikeda et al.[39] in acetonitrile.

**Competition between Nitrate and Chloride Ligands.** In sample I, the ratio of chloride and nitrate is the same, the latter originating from dissolved uranyl nitrate in $C_4$mim$Tf_2N$. As shown by EXAFS, addition of chlorides (from sample C to sample I) does not induce dissociation of nitrates from uranyl, but coordination of about one Cl atom. The resulting total equatorial CN decreases from 6 to 5, presumably because of steric hindrance, Cl atoms being bigger than O atoms. As on the average, 1 $Cl^-$ and

(46) Bhatt, A. I.; Kinoshita, H.; Koster, A. L.; May, I.; Sharrad, C.; Steele, H. M.; Volkovich, V. A.; Fox, O. D.; Jones, C. J.; Lewin, B. G.; Charnok, J. M.; Hennig, C.: In *Separations for the nuclear fuel cycle in the 21st century*, Proceedings ATALANTE; ACS Symposium Series: Nîmes, France, June 21−24, 2004.
(47) Thuery, P.; Nierlich, M.; Keller, N.; Lance, M.; Vigner, J.-D. *Acta Crystallogr.,Sect.C: Cryst. Struct. Commun.* **1995**, *51*, 1300.
(48) Alcock, N. W.; Kemp, T. J.; Leciejewicz, J. *Inorg. Chim. Acta* **1993**, *203*, 81.
(49) Berthet, J.-C.; Nierlich, M.; Ephritikhine, M. *Dalton Trans.* **2004**, 2814.
(50) Oldham, S. M.; Scott, B. L.; Oldham Junior, W. J. *Appl. Organomet. Chem.* **2006**, *20*, 39.
(51) Taylor, J. C.; Wilson, P. W. *Acta Crystallogr., Sect. B* **1973**, *29*, 1073.
(52) Nockemann, P.; Servaes, K.; Deun, R. V.; Hecke, K. V.; Meervelt, L. V.; Binnemans, K.; Görller-Walrand, C. *Inorg. Chem.* **2007**, *46*, 11335.

2 $NO_3^-$ are coordinated to uranyl, only 50% of the chlorides are thus complexed to uranyl in solution. The average coordination sphere given by EXAFS can be interpreted either by the formation of a unique species $UO_2Cl(NO_3)_2^-$ or by a mixture of several species in solution. Those experimental results are to be compared with simulation results. According to QM calculations, $Cl^-$ complexation by $UO_2(NO_3)_2$ is energetically favored in the gas phase. However, MD simulations, taking into account solvation and solvent−solvent interactions, are less conclusive and show that there is no strong driving force for complexing $Cl^-$ from the nitrato-complex in the IL solution.

The results given by EXAFS and UV−vis spectroscopies for sample J, containing an excess of chloride as compared to nitrate ions, are not fully consistent with each other. Actually, when a 4-fold (or more) excess of chloride ions was added to a uranyl solution of $C_4mimTf_2N$ in absence of nitrate (sample K), $UO_2Cl_4^{2-}$ species is formed according to EXAFS and UV−vis spectroscopies.[13,41] In the presence of nitrates, however, (sample J) EXAFS and UV−vis results give somewhat different information. EXAFS results can be interpreted by the formation of $UO_2Cl_4^{2-}$ with the same U−Cl distances as in non-aqueous solvents.[53] The UV−vis spectrum, however, does not display the fine structures observed for $UO_2Cl_4^{2-}$.[42] Furthermore, we note that the shape and intensity of this spectrum are affected by the presence of nitrate in the solution, but not by its concentration, at least for $[NO_3^-]/[UO_2^{2+}]$ ranging from 2 to 12. Even at the highest nitrate concentration, we do not evidence the formation of uranyl trinitrato complex. How to conciliate the EXAFS and UV−vis results? The EXAFS technique does not give a speciation in solution, but average distances of the uranyl neighbors, up to about 4 Å. Considering the uncertainties on the calculated coordination number, we can envision an equilibrium between different complexes involving $UO_2Cl_4^{2-}$ to be consistent with EXAFS results (∼3.5 Cl). The observed UV−vis spectrum would thus result from a mixture of $UO_2Cl_4^{2-}$ with other species, likely nitrato-complexes. This would be consistent with the high UV−vis absorption observed, as nitrato-species of uranyl absorb more strongly than $UO_2Cl_4^{2-}$ and thus can hide the signal of the latter. Interestingly, according to calculations in the gas phase and in solution, the most stable species to be formed is not $UO_2Cl_4^{2-}$ but the $UO_2Cl_3(NO_3)^{2-}$ complex that has also been characterized in the solid state.[54] A noticeable concentration of this complex would modify the UV−vis spectrum of the solution without drastically changing the average coordination sphere of uranyl, as detected by EXAFS.

Comparing the results obtained for samples J and P raises kinetics and thermodynamic equilibrium issues. Both samples contain the same IL and uranyl, nitrate, and chloride ions at the same ratio (1/2/6), but their preparation procedure was different: in sample J nitrates were introduced by dissolving the $UO_2(NO_3)_2$ salt, while in sample P they were introduced via the $C_4mimNO_3$ salt. The resulting UV-spectra (before adding $Cl^-$ anions) were similar and consistent with the average complexation of 2 nitrates per uranium, to form either $UO_2(NO_3)_2$ or/and a mixture of $UO_2(NO_3)^+$ and $UO_2(NO_3)_3^-$ species by dismutation of $UO_2(NO_3)_2$.[13] However, addition of the same amount of chlorides in those solutions surprisingly resulted in somewhat different UV−vis spectra. The amount of $UO_2Cl_4^{2-}$ species in solution P is clearly higher than in solution J, which would mean that the $UO_2(NO_3)_2$ complex formed in situ is more "reactive" than the one directly dissolved. Reactivity may also involve other nitrato-complexes like $UO_2(NO_3)^+$ or $UO_2(NO_3)_3^-$. Apart from the fabrication mode, solutions J and P differ by the nature of the chloride counterion: $TBA^+$ and $C_4mim^+$, respectively. In contrast to the former cation, $C_4mim^+$ can display H-bonding interactions with the complexed $Cl^-$ and $NO_3^-$ ligands and better stabilize a specific anionic complex.[55] It can be surmised, however, that the nature of the $Cl^-$ counterion has little effect on the process observed since it has no visible effect on the sole $Cl^-$ complexation in the IL (compare samples K and L). Slow kinetics may be related to the solvation patterns of ionic solutes in ILs which, according to MD calculations, are of "onion-shell" type with charge alternation around the central cation.[56,57] As a matter of fact, the solvation of the dinitrato-complex of uranyl in $C_4mimTf_2N$ involves the complexation of two $Tf_2N^-$, formally leading to an anionic complex surrounded by a second solvation shell, comprising about five $C_4mim^+$ cations. Such a solvation "structure" is expected to yield slow kinetics for anionic ligand exchange, raising equilibration issues. Similar kinetic problems have been pointed out by previous studies on the Eu(III) solvation in different ILs.[58]

## Conclusion

We have first carried out an extensive study of nitrate complexation to uranyl in a hydrophobic IL $C_4mimTf_2N$, as a function of the nitrates/uranyl ratio. In this medium the nitrates are found to behave as in organic solvents,[39] and we have evidenced in this work that at $NO_3$/U ratio from 1 to 3, their complexation is total.

By coupling experimental methods and molecular dynamics calculations, we have then investigated the competition between nitrate and chloride ions and shown that both are strong ligands to uranyl, of comparable strength in the IL. In fact, at low Cl/U ratio (2/1) and identical $Cl/NO_3$ ratio (2/2), uranyl forms mixed complexes like $UO_2Cl(NO_3)_2^-$. At higher Cl/U ratio (4 or higher) and different nitrate concentrations, uranyl forms a mixture of complexes, probably $UO_2Cl_3(NO_3)^{2-}$ and $UO_2Cl_4^{2-}$, even when nitrates are in excess over chlorides. Our results also hint for possible kinetic effects on the uranyl solvation and "reactivity" in the IL.

This study deals with two common ligands: nitrates and chlorides. In particular, the synthesis mode of ILs[59] entails

(53) Hennig, C.; Servaes, K.; Nockemann, P.; Hecke, K. V.; Meervelt, L. V.; Wouters, J.; Fluyt, L.; Görller-Walrand, C.; Deun, R. V. *Inorg. Chem.* **2008**, *47*, 2987.

(54) Indira, A.; Sridhar, M. A.; Qayyas, N. N. A.; Prasad, J. S.; Robins, W. T. *Z. Kristallogr.* **1994**, *209*, 916.

(55) For recent studies on the effect of IL cation of the stabilization of anionic metallic complexes, see: Chaumont, A.; Wipff, G. *Inorg. Chem.* **2009**, *48*, 4277–4289. Schurhammer, R.; Wipff, G. *J. Phys. Chem. B* **2007**, *110*, 4659–4668.

(56) Chaumont, A.; Wipff, G. *Inorg. Chem.* **2004**, *43*, 5891.

(57) Chaumont, A.; Wipff, G. *Chem.—Eur. J.* **2004**, *10*, 3919.

(58) Gaillard, C.; Billard, I.; Chaumont, A.; Mekki, S.; Ouadi, A.; Denecke, M. A.; Moutiers, G.; Wipff, G. *Inorg. Chem.* **2005**, *44*, 8355.

(59) Billard, I.; Mekki, S.; Gaillard, C.; Hesemann, P.; Moutiers, G.; Mariet, C.; Labet, A.; Bunzli, J. C. *Eur. J. Inorg. Chem.* **2004**, 1190.

that chlorides are the main impurity and are present unless caution has been paid to remove them. According to our studies, such ligands are not spectator ions, even when present at a low concentration, and can cause possible interference.

**Acknowledgment.** This work was supported by ACTINET and the GNR CNRS-PARIS. A.C. and W.G. are grateful to IDRIS, CINES, Université de Strasbourg for computer resources, and to Etienne Engler for assistance.